Characterization of the Output Pulses of a Simultaneous Q-Switched and Mode-Locked Intracavity Frequency-Doubled Diode-Pumped Pulsed Nd^{3+}-Laser

B. Abdul Ghani* and M. Hammadi

Atomic Energy Commission, P.O. Box 6091, Damascus, Syria

(Received March 7, 2011; in final form May 18, 2012)

A mathematical model for describing the polarization effect of the intracavity frequency-doubling of a simultaneous passively Q-switched and mode-locked diode-pumped Nd^{3+}-laser has been demonstrated. The generated polarized waves are assumed to be fixed through the lasing cycle. The maximum absorber initial transmission and the minimum mirror reflectivity values have been determined from the second threshold criterion. The calculated numerical results demonstrate the impact of the variation of the input laser parameters on the characteristics of the output laser pulses. The calculated results are in good agreement with the available experimental data reported in references.

PACS: 42.55Px, 42.55Rz, 42.68.Mj

1. Introduction

Intracavity frequency-doubling (IFD) lasers at wavelength 532 nm with high repetition rate, high peak power, and moderate average power could be of a great interest for simultaneous Q-switching and mode-locking processes. The output Nd^{3+}-laser pulse trains can be used in many applications such as under-water communication, medicine, active imaging, holography, information storage, and coherent communications [1, 2].

The green laser sources at wavelength 532 nm generally suffer from a large fluctuation in the output laser pulse, due to the coupling of different longitudinal modes through summing frequency mixing in the IFD crystal. The mode-locking process improves the average second harmonic (SH) power stability through eliminating the longitudinal mode-beating by making them oscillate in the same phase. This leads to a higher conversion efficiency which corresponds to a high peak power ultrashort output pulses at fundamental wavelength of 1.06 μm [3, 4].

In comparison with dye cells, the polarized isotropic Cr^{4+}:YAG crystal has good thermal and mechanical properties, due to its high threshold damage as well as its big relaxation time. When the pumping intensity is high enough, all of the Cr^{4+} ions are quickly excited to the first excited state. The strong excited state absorption accumulates great quantity of Cr^{4+} ions to the higher lying levels [4]. Since the relaxation time of the higher excited lying levels is relatively short (0.1 ns), a passive mode-locking process into the polarized isotropic Cr^{4+}:YAG crystal is possible. If strong intensity fluctuations are introduced, the build-up time of pulse will be sufficiently short [5]. The pulse build-up time can be sufficiently shortened by putting the saturable absorber at a tight spot size location inside the cavity. The fundamental Q-switched and simultaneous mode-locked output laser pulse can then be performed [4, 5].

The problem of passively Q-switched lasers with simultaneous mode-locking has been treated experimentally and theoretically in many references [1, 4–9] with, and without the existing of the IFD. The mentioned references did not treat the impact of the polarization process on the characteristics of the output laser pulse.

When the saturation absorption in Cr^{4+}:YAG becomes significant, the polarization characteristics can be formed at the stage of growth of a giant laser pulse. The self-induced polarization anisotropy in the cavity appears due to the self-induced anisotropy of the saturation absorption and the self-induced changes in polarization within the cavity. Changing the angular position of Cr^{4+}:YAG switch in the cavity altered the degree of ellipticity of the polarization. The appearance of the polarization ellipticity ε is related to the self-induced birefringence in the Cr^{4+}:YAG crystal during the stage of the absorption saturation.

A general recurrence formula has been derived in [10] in order to analyze the temporal shape behavior of a single Q-switched envelope with mode-locking pulse trains.

This work offers a simple methodology for deduction the second threshold of Q-switched operation. The influence of the intracavity focusing, excited state absorption, IFD, and the presence of a polarized Cr^{4+}:YAG crystal have been taken into consideration in the developed mathematical model. Moreover, a criterion for the formation of the giant laser pulse has been also determined. Determining the output pulse characteristics such as maximum peak energy and build-up time for different values of the absorber initial transmission is another interest of this work.

2. Mathematical model

2.1. Q-switching process

When the polarized Cr^{4+}:YAG saturable absorber is saturated before the gain, the photon density increases

* corresponding author; e-mail: pscientific@aec.org.sy

and generates alternative giant output laser pulses. If the gain is saturated before the absorber, then the photon density never increases sufficiently to develop a giant output laser pulse [4, 7]. We assume that the pumping gain medium is uniform and the densities in gain and polarized Cr^{4+}:YAG saturable absorber are also axially uniform. We neglect the spontaneous emission of the gain medium and consider the influence of intracavity focusing, the excited state absorption, IFD and the polarization effect (Figs. 1 and 2).

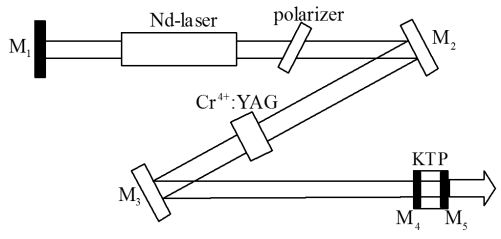

Fig. 1. Experimental setup of the IFD simultaneously Q-switched and mode-locked diode-pumped Nd^{3+}-laser with polarized Cr^{4+}:YAG saturable absorber [3].

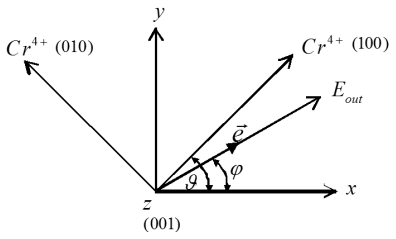

Fig. 2. Angular orientations of Cr^{4+}:YAG crystal axes (ϑ, $\vartheta+\pi/2$) and polarization angle of the electrical field $E_{\rm out}(\varphi)$ (with resonantly absorbing dipoles) of the pumping output laser pulse.

The following rate equations describe the fundamental photon density, population density of the gain medium and population inversion density of the ground state of the polarized absorber [1, 4, 5, 7–13]:

$$\frac{\mathrm{d}U_Q}{\mathrm{d}t} = \frac{U_Q}{t_r}\Big\{\big[2\sigma N\ell - 2\sigma_{GS}N_1^s\ell_s\cos^2(\vartheta-\varphi) - 2\sigma_{ES}N_2^s\ell_s\sin^2(\vartheta-\varphi)\big] - \Big[\ln\Big(\frac{1}{R}\Big) + \rho_{ns} + \alpha_x\cos^2\varphi + \alpha_y\sin^2\varphi\Big] - \eta_{2\omega}vW_pU_Q\Big\}, \tag{1}$$

$$\frac{\mathrm{d}N}{\mathrm{d}t} = -\gamma\sigma cU_QN, \tag{2}$$

$$\frac{\mathrm{d}N_1^s}{\mathrm{d}t} = -\frac{Ac}{A_s}\sigma_{GS}U_QN_1^s\cos^2(\vartheta-\varphi). \tag{3}$$

Full details about this mathematical model are demonstrated in [10].

Presence of $\cos^2(\vartheta-\varphi)$ and $\sin^2(\vartheta-\varphi)$ functions in Eqs. (1) and (3) makes the mathematical model essentially sensitive to the self-induced anisotropy appearing in the nonlinear stage of the giant output pulse formation [6, 14]. For the anisotropic Nd:YVO_4 active medium, the generated polarized waves with resonantly absorbing dipoles are fixed through the lasing cycle.

The orientations of the x and y axes are chosen so that the total cavity loss is in its minimum along x axis and in its maximum along y axis. The axes [100] and [010] (Fig. 2) are oriented with respect to the optical axis z [001] at the angle ϑ and $\vartheta+\pi/2$, respectively [6]. Suppose that the cuts of YAG crystalline host is positioned in the cavity along (100), so that the light propagates along (100) crystallographic axis, while the laser polarization azimuth is kept fixed (given by the orientation of the Nd:YVO_4) and, of course, orthogonal to this direction [14] (Fig. 2).

Dividing Eq. (1) by Eq. (2), and considering that $N_1^s(t_k)+N_2^s(t_k)=N_0^s$ and $N_1^s(t_k)=N_0^s\Big[\frac{N(t_k)}{N_i}\Big]^{\xi}$, it can be followed that:

$$\frac{\mathrm{d}U_Q}{\mathrm{d}N} = -\frac{\ell}{\gamma L_{\rm eff}}\Big\{1+\frac{\beta}{2\sigma N_i\ell}\ln\frac{1}{T_0^2}\Big(\frac{N}{N_i}\Big)^{\xi-1} - \frac{1}{2\sigma N_i\ell}\cot^2(\vartheta-\varphi)\ln\frac{1}{T_0^2}\Big(\frac{N}{N_i}\Big)^{\xi-1} - \frac{1}{2\sigma N\ell}\beta\ln\frac{1}{T_0^2} - \frac{1}{2\sigma N\ell}\Big[\ln\Big(\frac{1}{R}\Big)+\rho_{ns} + \alpha_x\cos^2\varphi+\alpha_y\sin^2\varphi\Big] - \frac{\eta_{2\omega}vW_p}{2\sigma N\ell}U_Q\Big\}, \tag{4}$$

where $T_0=\exp(-\sigma_{GS}N_0^s\ell_s\sin^2(\vartheta-\varphi))$ is the polarized absorber initial transmission, $\beta=\sigma_{ES}/\sigma_{GS}$, $\xi=\frac{\sigma_{GS}}{\sigma\gamma}\frac{A}{A_s}\cos^2(\vartheta-\varphi)$ and

$$\varphi = \vartheta - \arcsin\Big(\sqrt{\ln(1/T_0)/\sigma_{GS}N_0^s\ell_s}\Big). \tag{5}$$

By integrating Eq. (5), the photon laser density can be given as follows:

$$U_Q = B_1N + B_2N^{\xi} - B_3, \tag{6}$$

where

$$B_1 = \frac{-2\sigma\ell}{2\sigma\gamma L_{\rm eff}-\eta_{2\omega}vW_p},$$

$$B_2 = \frac{-\beta\ln(1/T_0^2)+\ln(1/T_0^2)\cot^2(\vartheta-\varphi)}{N_i^{\xi}(2\sigma\gamma L_{\rm eff}-\eta_{2\omega}vW_p)},$$

$$B_3 = \frac{\beta\ln(1/T_0^2)+\ln(1/R)+\rho_{ns}+\alpha_x\cos^2\varphi+\alpha_y\sin^2\varphi}{\eta_{2\omega}vW_p},$$

where N_i is the initial population inversion density. Generally, by setting $N=N_i$, $N_1^s=N_0^s$ and $\frac{\mathrm{d}U_Q}{\mathrm{d}t}=0$ in Eq. (1), the initial population inversion density can be given by the following relation:

$$N_i = \frac{1}{2\sigma\ell}\big[\ln(1/T_0^2)+\ln(1/R)+\rho_{ns} + \alpha_x\cos^2\varphi+\alpha_y\sin^2\varphi\big]. \tag{7}$$

The output pulse energy at the fundamental and SH wavelength are given by the relation [1, 4, 7, 10]:

$$E_\omega = \frac{AW_p}{2\sigma}\ln\left(\frac{1}{R}\right)\sum_{k=0}^{\infty}U_k,$$
$$E_{2\omega} = \frac{W_p}{\sigma}\frac{A^2}{A_c}\rho_{\mathrm{KTP}}\sum_{k=0}^{\infty}U_k^2. \tag{8}$$

The Q-switching process can be achieved using the second derivative of U_Q with positive or negative sign. If positive, then the photon density can grow. Now using (4), the second derivative of the photon density U_Q is given as follows:

$$\frac{\mathrm{d}^2U_Q}{\mathrm{d}N^2} = -\frac{\ell}{\gamma L_{\mathrm{eff}}}\left\{\frac{\beta(\xi-1)}{2\sigma N_i^2\ell}\ln\frac{1}{T_0^2}\left(\frac{N}{N_i}\right)^{\xi-2}\right.$$
$$-\frac{\xi-1}{2\sigma N_i^2\ell}\cot^2(\vartheta-\varphi)\ln\frac{1}{T_0^2}\left(\frac{N}{N_i}\right)^{\xi-2}$$
$$+\frac{\beta}{2\sigma N^2\ell}\ln\frac{1}{T_0^2}+\frac{1}{2\sigma N^2\ell}\left[\ln\left(\frac{1}{R}\right)+\rho_{ns}\right.$$
$$\left.+\alpha_x\cos^2\varphi+\alpha_y\sin^2\varphi\right]+\frac{\eta_{2\omega}vW_p}{2\sigma N^2\ell}U_Q$$
$$\left.-\frac{\eta_{2\omega}vW_p}{2\sigma N\ell}\frac{\mathrm{d}U_Q}{\mathrm{d}N}\right\}. \tag{9}$$

Then, the criterion of formation of a giant Q-switched output laser pulse ($N = N_i$) will be

$$\left[-\beta(\xi-1)+(\xi-1)\cot^2(\vartheta-\varphi)-\beta\right]\ln\left(\frac{1}{T_0^2}\right)$$
$$>\left[\ln\left(\frac{1}{R}\right)+\rho_{ns}+\alpha_x\cos^2\varphi+\alpha_y\sin^2\varphi\right]. \tag{10}$$

Therefore

$$T_0^{\max} < \exp\left(\frac{\ln(1/R)+\rho_{ns}+\alpha_x\cos^2\varphi+\alpha_y\sin^2\varphi}{2\left[\beta(\xi-1)-(\xi-1)\cot^2(\vartheta-\varphi)+\beta\right]}\right). \tag{11}$$

On the other hand, the reflectivity of the output mirrors should have a lower value to build-up a giant output laser pulse for limited values of ρ_{ns} and T_0. Using (10), the output mirror reflectivity should then satisfy the following inequality:

$$R^{\min} > \exp\Big(\big(\beta(\xi-1)-(\xi-1)\cot^2(\vartheta-\varphi)+\beta\big)$$
$$\times\ln(1/T_0^2)+\big(\rho_{ns}+\alpha_x\cos^2\varphi+\alpha_y\sin^2\varphi\big)\Big). \tag{12}$$

It is important to mention here that the parameters involved in Eq. (11) such as β, T_0, R, α_x, α_y, ρ_{ns} ... etc. are essential parameters in designing the passively Q-switch device, laser rod and the resonator [4].

2.2. Mode-locking process

A desirable condition for a good-pulsed mode-locking is that the saturable absorber should have enough short lifetime to recover its absorption process between individual noise bursts. Under this condition, the preferred pulse does not bring up several closely following noise spikes along with it.

The relaxation time is in the microsecond region, which generally would not be allowed to obtain mode-locking. Nevertheless, when the intracavity intensity is high enough, all of the Cr^{4+} ions are quickly excited to the first excited state, and strong excited state absorption causes a great quantity of Cr^{4+} ions to accumulate in higher-lying levels. The relaxation time of the excited state absorption is relatively short ($\tau_{es} = 0.1$ ns) [4]. Passive mode-locking with a Cr^{4+}:YAG saturable absorber would be possible if strong intensity fluctuations are introduced. Another important condition is that the build-up time of the Q-switched pulse must be sufficiently short due to the limitation of the round trip time of the density fluctuation [4].

The phenomena of mode-locking in a passive Q-switched laser pulse achieved by polarized solid state Cr^{4+}:YAG saturable absorber can be explained by the fluctuation mechanism. There are two stages of the pulse formation: the linear stage of the laser intensity fluctuation is generated due to the interference of a large number of modes in the cavity, and the nonlinear stage is referred to the bleaching process in the polarized Cr^{4+}:YAG saturable absorber. The most compressed intensive fluctuation laser peaks can be amplified faster than the weaker ones in the nonlinear stage [1, 5, 7]. The nonlinear parameter, related to the pulse compression in the nonlinear stage, is given by the following relation [4]:

$$\mu = \frac{1-\exp\left(-\sigma_{GS}N_0^s\ell_s\sin^2(\vartheta-\varphi)\right)}{t_b(\mathrm{d}\alpha/\mathrm{d}t)}, \tag{13}$$

where $\mathrm{d}\alpha/\mathrm{d}t$ is the gain increment speed at threshold pumping time.

The pulse build-up time t_b can be estimated by the following relation, only when it is shorter than the absorber upper-level lifetime [2, 4]:

$$t_b = (25\pm5)t_rC_b, \tag{14}$$

where $C_b = \frac{N_{\mathrm{th}}}{\ln(1/R)(N_i-N_{\mathrm{th}})}$ is the build-up time coefficient and N_{th} is the threshold inversion density exactly after the absorber bleaching.

The value of N_{th} depends on the final transmission of the polarized Cr^{4+}:YAG saturable absorber. The final transmission of the saturable absorber is given by the following relation [2]:

$$T_f = \exp\left(-\beta\sigma_{GS}N_0^s\ell_s\sin^2(\vartheta-\varphi)\right). \tag{15}$$

Using (4), the threshold of the population inversion density, after bleaching process of the polarized Cr^{4+}:YAG saturable absorber, is given as follows (for $\frac{\mathrm{d}U_Q}{\mathrm{d}N}(N = N_{\mathrm{th}}) = 0$):

$$N_{\mathrm{th}} = \frac{1}{2\sigma\ell}\big(\ln(1/T_f^2)+\ln(1/R)+\rho_{ns}$$
$$+\alpha_x\cos^2\varphi+\alpha_y\sin^2\varphi\big). \tag{16}$$

3. Results and discussion

The calculated results, in this work, are generated using the parameters values reported in Table 1 [10]. Figure 3 demonstrates the dependence of the pulse build-up time coefficient on the absorber initial transmission for several values of the output mirror reflectivity at rotational angle of 65°. When the absorber initial transmis-

sion is low, the build-up time for a given output reflectivity is short. The build-up time can also be shortened by decreasing the output reflectivity. However, a lower output mirror reflectivity results in a higher threshold. Therefore, the output reflectivity should be chosen higher than 50% for pulse mode-locking.

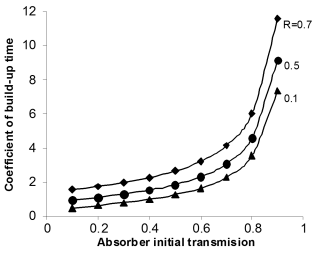

Fig. 3. Coefficient of pulse build-up time versus the absorber initial transmission for several values of the output mirror reflectivity and for rotational angle of 65°.

Figure 4 shows the output peak energy of a single Q-switched envelope and the SH peak energy versus the absorber initial transmission for two values of the output mirror reflectivity at 65° of rotational angle. By increasing the absorber initial transmission, the output peak energy and the SH peak energy decrease due to the KTP crystal high losses and to a limitation of the conversion efficiency.

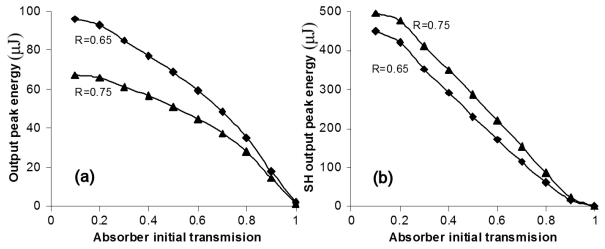

Fig. 4. Maximum output energy of a single Q-switched envelope (a) and SH pulses (b) versus the absorber initial transmission for two values of the output mirror reflectivity and for rotational angle of 65°.

Figure 5 shows the calculated results of SH output pulse energy versus A/A_s for several values of absorber initial transmission, 75% of output mirror reflectivity and 65° of rotational angle. Initially, the SH output pulse energy rises as the ratio A/A_s increases. It can be seen from Fig. 5 that the SH output pulse energy saturates faster for a smaller value of absorber initial transmission.

Figure 6 shows the SH peak power of central mode as a function of rotational angle of the polarized Cr^{4+}:YAG isotropic crystal for different values of the absorber initial transmission. It is shown in this figure that at high laser transmission, the maximum SH peak power tends closely to isotropic state. The decrement of the absorber initial transmission leads to the increment in the SH peak power. Then, the optical Cr^{4+} active centers become

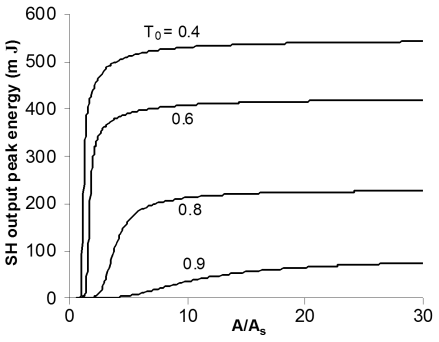

Fig. 5. SH output pulse energy versus A/A_s for several values of the absorber initial transmission, 0.75 of output mirror reflectivity and 65° of rotational angle.

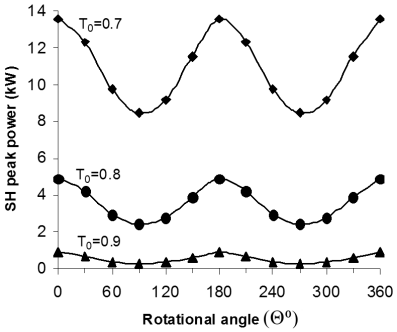

Fig. 6. Central mode SH peak power versus polarized crystal rotational angle for different values of initial transmission.

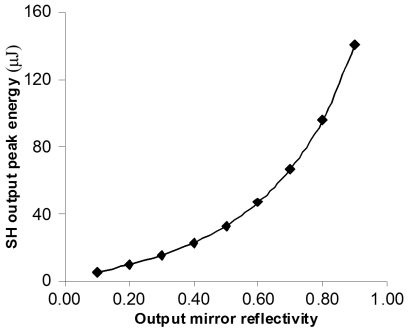

Fig. 7. SH output peak energy versus the output mirror reflectivity.

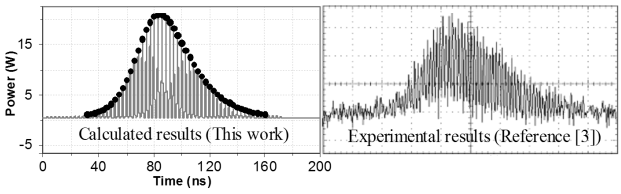

Fig. 8. Calculated and experimental results of the Q-switched pulse power at fundamental wavelength, which leaked through the high-reflectivity mirror. $T_0 = 0.81$.

steadily saturated and the anisotropic behavior clearly appears. As the laser radiation propagates along [001] optical axis (Fig. 2), the power required for saturation must be at its maximum. This happens when the transition is at its minimum and the SH power is at its maximum. This means that the electric vector is parallel to either [010] or [100] transition moments for $\vartheta = 0°$, 180°, and 360°, respectively. In this case, only one subset (one-third) of the total active centers participates in the laser action; and for $\vartheta = 90°, 270°$ two subsets (two--third) of the total active centers with [010] and [100] transition moments are simultaneously participating in the laser action. This qualitatively interprets the behavior peaks and troughs appearing in Fig. 6.

Figure 7 demonstrates the dependence between the SH output peak energy and the output mirror reflectivity. By increasing the output mirror reflectivity, the SH output peak energy nonlinearly increases. The nonlinear increment may be due to the high losses in the laser cavity (linear absorption loss, transmission loss at the mirror, polarization rotation loss and in general high loss by KTP).

Finally, Fig. 8 shows a comparison between the calculated, in this work, and experimental results reported in [3] for the fundamental Q-switched pulse power, which leaked through the high-reflectivity mirror. Good agreement can be seen between both pulse profiles. The calculated pulse width of the Q-switched envelope reaches 65 ns in this work, whereas the experimental value reported in Ref. [3] is 70 ns. The slight mismatch may be due to the inaccuracy in estimating the intracavity losses.

4. Conclusion

This work presents a mathematical model to describe the use of a polarized Cr^{4+}:YAG saturable absorber as a tool of passively Q-switched simultaneously mode-locked including IFD and Fresnel losses. This model is essentially sensitive to the self-induced anisotropy appearing in the Cr^{4+}:YAG saturable absorber during the nonlinear stage of the giant pulse formation.

A mathematical methodology based on second threshold criterion has been derived to determine the maximum absorber initial transmision and the minimum mirror reflectivity values. The numerical calculations show that low values of the absorber initial transmission are beneficial in generating high power Q-switched mode-locked SH laser pulses. The calculated numerical results show a good consistency with the available experimental data.

The proposed mathematical model can be applied to investigate other Nd-lasers such as Nd:YAG and Nd:$GdVO_4$.

Acknowledgments

The authors would like to express their thanks to the Director General of AECS Prof. I. Othman for his continuous encouragement, guidance and support.

References

[1] P.K. Mukhopadhyay, M.B. Alsous, K. Ranganathan, S.K. Sharma, P.K. Gupta, J. George, T.P.S. Nathan, *Appl. Phys. B, Lasers Opt.* **79**, 713 (2004).

[2] P.K. Mukhopadhyay, M.B. Alsous, K. Ranganathan, S.K. Sharma, P.K. Gupta, A. Kuruvilla, T.P.S. Nathan, *Opt. Laser Technol.* **37**, 157 (2005).

[3] P.K. Mukhopadhyay, M.B. Alsous, K. Ranganathan, S.K. Sharma, P.K. Gupta, J. George, T.P.S. Nathan, *Opt. Commun.* **222**, 399 (2003).

[4] Y.F. Chen, S.W. Tsai, *IEEE J. Quant. Electron.* **37**, 580 (2001).

[5] Y.F. Chen, J.L. Lee, H.D. Hsieh, S.W. Tsai, *IEEE J. Quant. Electron.* **38**, 312 (2002).

[6] B. Abdul Ghani, M. Hammadi, *Acta Phys. Pol. A* **115**, 873 (2009).

[7] Y.F. Chen, Y.P. Lan, H.L. Chang, *IEEE J. Quant. Electron.* **37**, 460 (2001).

[8] J. Liu, D. Kim, *IEEE J. Quant. Electron.* **35**, 1724 (1999).

[9] J. Liu, D. Shen, S.C. Tam, Y.L. Lam, *IEEE J. Quant. Electron.* **37**, 888 (2001).

[10] B. Abdul Ghani, M. Hammadi, *Acta Phys. Pol. A* **122**, 103 (2012).

[11] J.J. Degnan, *IEEE J. Quant. Electron.* **31**, 1890 (1995).

[12] Y.S. Huang, F.L. Chang, *Opt. Rev.* **12**, 396 (2005).

[13] G. Li, S. Zhao, K. Yang, J. Liu, *Opt. Mater.* **27**, 719 (2005).

[14] E.R Villiafana, A.V. Kir'yanov, *Opt. Commun.* **242**, 241 (2004).